THE ASTROPHYSICAL JOURNAL, 356:110–118, 1990 June 10

EINSTEIN X-RAY OBSERVATIONS OF M101

G. TRINCHIERI,[1,2] G. FABBIANO,[1] AND S. ROMAINE[1]

Received 1989 September 11; accepted 1989 December 12

ABSTRACT

We present the *Einstein* X-ray observations of the face-on spiral galaxy M101. The global X-ray luminosity of M101 is $L_x \sim 1.2 \times 10^{40}$ ergs s^{-1} for $D = 7.2$ Mpc, consistent with the expected X-ray luminosity of normal spiral galaxies of its optical magnitude. The X-ray emission is mostly due to very luminous individual sources, with $L_x > 10^{38}$ ergs s^{-1} each, most likely very massive accreting binary systems. The data suggest a deficiency of sources in the luminosity range of $L_x \sim 10^{37-38}$ ergs s^{-1}, which would indicate that the luminosity distribution of the X-ray sources in M101 might be different from that of M31 or M33.

Subject headings: galaxies: individual (M101) — galaxies: stellar content — galaxies: X-rays — luminosity function

I. INTRODUCTION

The X-ray observations obtained with the *Einstein* Observatory (see Giacconi *et al.* 1979 for a description of the satellite) have shown that nearby spiral galaxies emit X-rays, mostly produced by many individual sources similar to those observed in the Milky Way (see Fabbiano 1989, and references therein). In several objects, these sources can be observed directly, and their spectral characteristics and temporal behavior indicate a large fraction of bright, close accreting binary systems and supernova remnants. For most other galaxies, only the integrated contribution of these sources can be observed as an extended emission, and this appears to be tightly correlated with the blue emitting stellar population, both in terms of a constant relative percentage of emission in spirals of all morphological types and luminosities, and in terms of a very similar radial distribution of X-ray and optical sources in spiral disks.

In this paper we report the study of the X-ray morphology, spectrum and source variability of the face-on Sc galaxy M101. This spiral galaxy has been extensively studied to obtain a calibration to the distance scale (Sandage and Tamman 1974). Its distance, estimated at 3.5 Mpc (Sandage 1962), has then been revised to 7.2 Mpc (Sandage and Tamman 1974) and 5.6 Mpc (Bottinelli and Gouguenheim 1976), making the H II regions in M101 among the brightest and largest observed. Long and Van Speybroeck (1983) have presented a brief discussion of the high luminosity and time variability of the X-ray sources in M101. McCammon and Sanders (1984) have performed a careful analysis of the *Einstein* X-ray data of M101, to constrain the amount of hot interstellar medium (ISM) present. Their upper limit to this emission sets severe constraints to models that predict the conversion of the Supernova energy deposition in spiral disks into observable diffuse X-ray emission (Cox and McCammon 1986).

The purpose of this work differs from the previous study of the X-ray emission in M101, since we are interested in all the components and not just the hot phase of the ISM, and we study the morphology and spectral and temporal characteristics of the X-ray emission. The details of our analysis and the results are given in the following section. A discussion of our results is summarized in § III.

[1] Harvard-Smithsonian Center for Astrophysics.
[2] Osservatorio Astrofisico di Arcetri.

II. DATA ANALYSIS AND RESULTS

M101 was observed twice with the *Einstein* imaging proportional counter (IPC), as summarized in Table 1. The two IPC images were processed with the latest version of the *Einstein* processing analysis system (Harnden *et al.* 1984). The field background was subtracted using the templates calculated by this software (see Fabbiano and Trinchieri 1987) in three energy bands (soft [0.2–0.8 keV], hard [0.8–3.5 keV], and broad [0.2–3.5 keV]) using a combination of IPC source-free deep survey fields plus a "Bright Earth" component to account for contamination by scattered solar X-ray photons. The normalization to the respective images is on average within an uncertainty of $\lesssim 20\%$ (see Harnden *et al.* 1984).

To improve the statistical significance in the analysis of the nonvariable components, we have also co-added the two IPC observations of M101 and analyzed the resulting merged image independently. The background for this field has been obtained by summing the templates of each individual IPC field.

For completeness, in Table 2, we also list a high resolution imager (HRI) observation pointed at M101. However, the HRI observation is very short, and it does not provide additional useful information on the X-ray emission from M101.

a) Contour Plots

The background subtracted images were used to produce the isointensity contour plots shown in Figures 1 and 2. A large region of extended, rather amorphous emission, can be seen at the center of the maps, along with several bright individual sources outside this region. No bright, point-like source is detected at the galactic center.

As already noticed by McCammon and Sanders (1984), the soft- and hard-energy band maps of M101 (shown in Fig. 2) are different. The hard band emission in the inner $\sim 5'$ is mostly clustered in two sources plus some more diffuse emission, while the soft maps show one extended central source. Several of the individual sources in the outer regions are mostly seen in the hard-band map.

The X-ray centroid (determined from the broad-band data) does not coincide with estimates of the center of M101 at other wavelengths, with differences of the order of a few arcmin. It should be noted however that different authors (McCutcheon 1973; Israel, Goss, and Allen 1975; Hutchmeier and Witzel

TABLE 1

OBSERVATIONS LOG

Sequence Number	Instrument	Live Time (s)	Date	Field Center R.A.	Field Center Decl.
2140.....	IPC	10383	79 Jan 6	$14^h1^m29^s.96$	54°36′00″
2141.....	IPC	6074	79 Jun 16	14 1 29.96	54 36 00
2899.....	HRI	2786	79 Dec 31	14 1 29.96	54 36 00

1979; Israel 1980) quote different coordinates for the center of M101, which can differ as much as ~2′.

The comparison of the maps in Figure 2 also indicates that the intensity of four sources plus the central peak has changed in the six months interval between the two observations. A quantitative estimate of the variations is given in the next section.

b) Individual Sources

i) *Source Luminosities*

The standard processing software detects several sources in M101. However, a comparison with the X-ray maps (Figs. 1–2) shows that some of the detections within ~3′–4′ from the center might be clumps in the diffuse emission. We have therefore produced a list of sources (Table 2) from a combination of the standard detect results and of a visual inspection of the merged X-ray maps. We have also estimated the intensity of the emission near the galaxy's center at the broad-band X-ray centroid. The count rates are obtained in a circle of 90″ radius (similar in area to the detection cell of the standard processing) in the broad band and are corrected for mirror scattering, dead time, point-spread function (PSF), and vignetting (Harnden *et al.* 1984). The errors are statistical only.

The background has been obtained from the templates discussed above. This choice might artificially enhance the X-ray count rate attributed to each source by including in the source counts some of the emission from the galaxy's disk (e.g., Trinchieri, Fabbiano, and Peres 1988). However, the present data do not show on average a significant excess over the expected background from the template outside of a radius of ~5′ (see McCammon and Sanders 1984).

We have decided to estimate the source counts in a smaller area than previously used for other galaxies (see, for example, the analysis of M33, Trinchieri, Fabbiano, and Peres 1988;

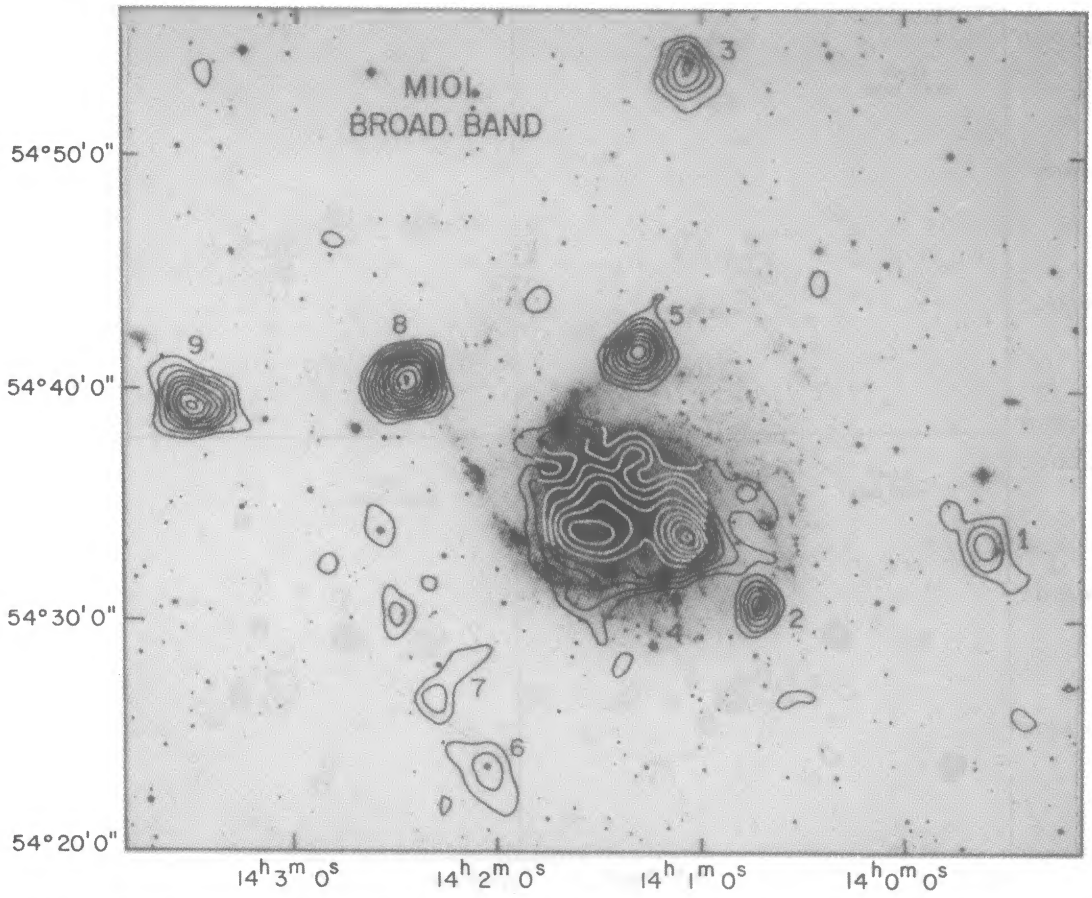

FIG. 1.—The X-ray isointensity contours superposed onto an optical picture of M101. The X-ray data are in the broad-energy band from the merged IPC image (*see text*), and have been smoothed with a Gaussian function of $\sigma = 32''$. Contours start at the 2 σ level above background.

TABLE 2

OBSERVED COUNT RATES OF THE X-RAY SOURCES IN M101

Source Number	X-Ray Position (1950)	I2140 Count Rate ($\times 10^{-3}$)	I2140 Error	I2141 Count Rate ($\times 10^{-3}$)	I2141 Error
1	$13^h59^m36^s.9$ 54°33′16″	IPC Ribs		4.6	1.7
2	14 00 43.6 54 30 52	3.9	1.3	3.2	1.5
3	14 01 05.7 54 54 03	5.4	1.5	6.3	1.9
4	14 01 06.3 54 33 41	13.3	1.7	8.0	1.8
5	14 01 20.0 54 41 47	9.3	1.5	4.6	1.6
Center	14 01 32.9 54 33 46	9.0	1.4	10.3	1.8
6	14 02 03.7 54 24 08	<5.8[a]		5.8	1.7
7	14 02 20.0 54 26 39	3.0	1.2	<4.3	
8	14 02 27.5 54 40 34	11.2	1.6	18.8	2.5
9	14 03 27.3 54 39 39	4.4[b]	1.4	24.0	3.0
10	14 03 54.8 54 25 18	>11.2[c]	1.9	<5.0	

[a] Detected in the hard band only, with a count rate of $3.0 \pm 1.0 \times 10^{-3}$.
[b] Not detected by the standard detect in this observation.
[c] Some shadowing from the IPC window support (*see text*).

M83, Trinchieri, Fabbiano, and Palumbo 1985) to maximize the statistical significance of the sources, although with this choice we have to use a large PSF correction (of ~33%). A larger area for the source counts (3′ radius circle) does not change significantly the count rates of most sources, except for sources number's 4, 6, and 7 (and of the central peak). These discrepancies are too large to be accounted for by the uncertainty in the PSF correction factor, which suggests that there is a residual low-level extended emission (evident for source number 4, but not for the other ones), more of which is included when the larger area is considered. The smaller detection cells should therefore include fewer counts from the galactic emission. With the present data, we cannot obtain a more accurate count rate for these sources apparently embedded in a

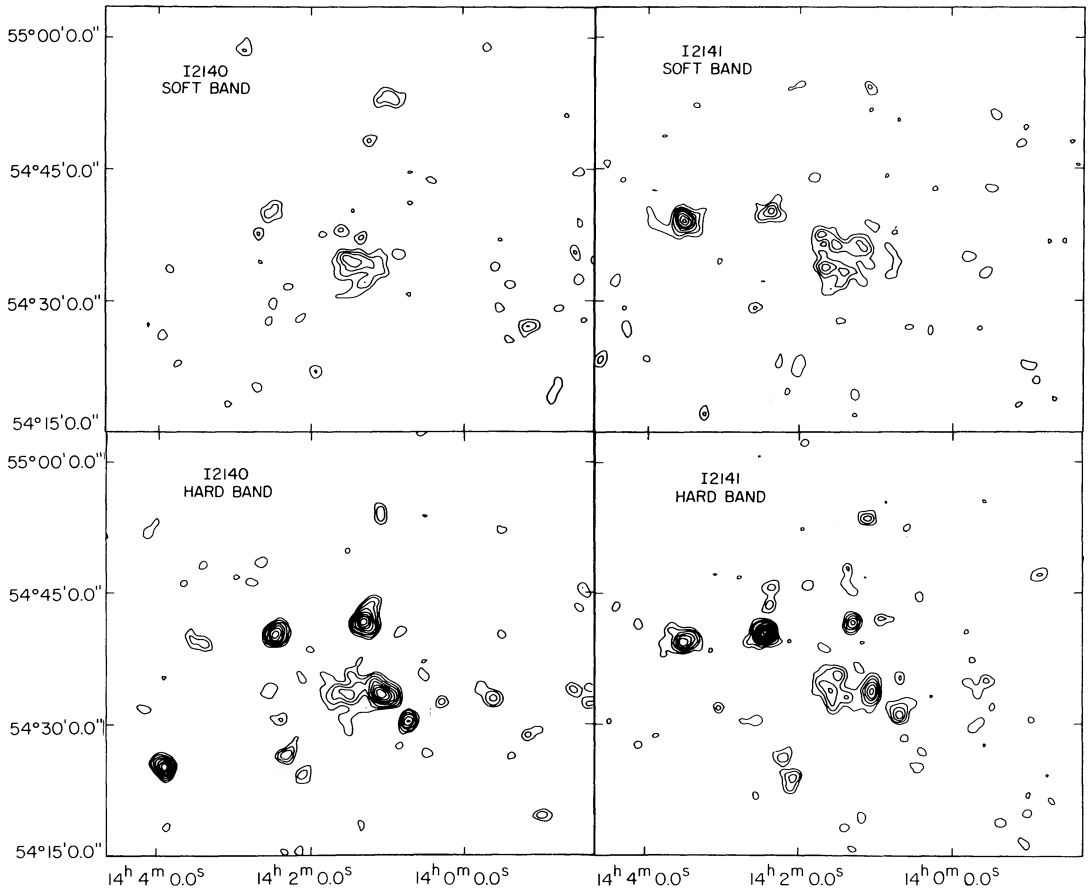

FIG. 2.—X-ray maps in the soft- and hard-energy band for the two IPC observations. A Gaussian function with $\sigma = 32''$ has been used to smooth the data. Contours start at 2 σ over the background.

TABLE 3

AVERAGE X-RAY FLUXES AND LUMINOSITIES OF THE SOURCES IN M101

Source Number	X-Ray Position (1950)	X-Ray Flux (ergs cm^{-2} s^{-1})	X-Ray Luminosity (ergs s^{-1})	Notes or Identification
1	$13^h59^m36^s.9$ 54°33′16″	1.5×10^{-13}	(9.2×10^{38})	Outside optical image of M101
2	14 00 43.6 54 30 52	1.0×10^{-13}	6.3×10^{38}	H II region NGC 5447
3	14 01 05.7 54 54 03	1.2×10^{-13}	...	SAO Star number 28988
4	14 01 06.3 54 33 41	3.7×10^{-13}	2.3×10^{39}	Between Sources 25 and 26 (OB/H II regions) 1
5	14 01 20.0 54 41 47	2.5×10^{-13}	1.6×10^{39}	OB/H II Complex 34 in 1
Center	14 01 32.9 54 33 46	3.0×10^{-13}	1.9×10^{39}	
6	14 02 03.7 54 24 08	6×10^{-14}	...	Star 2 Source 57 in 1
7	14 02 20.0 54 26 39	7.3×10^{-14}	4.6×10^{38}	Radio Source WE1402+54W2 3
8	14 02 27.5 54 40 34	4.5×10^{-13}	2.8×10^{39}	S12 4, 64 in 1
9	14 03 27.3 54 39 39	3.5×10^{-13}	1.3×10^{43}	QSO 5
10	14 03 54.8 54 25 18	$>2.6 \times 10^{-13}$	(1.6×10^{39})	Radio Sources WE1403+54W1 WE1403+54W2 3

NOTES.—The flux of source number 1 is obtained from the I2141 data only. X-ray fluxes and luminosities (0.2–4.0 keV) are for a thermal bremsstrahlung spectrum with kT = 5 keV and $N_H = 1.2 \times 10^{20}$ cm^{-2} (galactic value, Stark *et al.* 1990) and $D = 7.2$ Mpc (Sandage and Tamman 1974), except for sources numbered 3 and 6, for which a thin plasma with metallic line spectrum is used. Source number 3 is at ~22″ from a galactic G star of $m_v = 7.2$, from which we derive $f_x/f_{opt} = 2.7 \times 10^{-5}$ (see Topka *et al.* 1982), consistent with values observed for other stars of similar spectral class. An estimate of the optical magnitude of the star positionally consistent with source number 6, based on its size on the Palomar Sky Survey print, gives ~10.7 mag. in the red band, from which we derive $f_x/f_{opt} \sim 3.4 \times 10^{-4}$, in the range of ratios observed for main sequence stars (Vaiana *et al.* 1981). The IPC error circles for sources numbers 7 and 10 contain one and two radio sources, respectively (within <45″ of the X-ray position). Israel, Goss, and Allen 1975 indicate that these sources are outside the optical image of M101 and are not identified with optical counterparts on the Palomar Sky Survey prints. Source number 7, however, could also be in a faint, outer spiral arm of M101, and not the X-ray counterpart of the radio source. Source number 9 is a highly variable low-luminosity AGN. This source will be discussed in Trinchieri, Fabbiano, and Elvis (1989).

REFERENCES.—(1) Hill, Bohlin, and Stecher 1984; (2) Allen and Goss 1979; (3) Israel, Goss, and Allen 1975; (4) Searle 1971; (5) Margon, Downes, and Chanan 1985.

more diffuse emission. It is likely, however, that the X-ray peaks observed in M101 are really individual sources, since in some of them a variation in the flux level might be observed (see below).

Four sources were detected in only one of the observations (numbers 7 and 10 in I2140 only, numbers 1 and 9 in I2141 only). An estimate of the count rate in the corresponding region of the other field has been obtained and 3 σ upper limits are given for these sources. Both sources numbers 1 and 10 fall in the IPC window support area (the "ribs") in the first IPC observation, where the estimate of the source flux is hampered by the unknown shadowing factor of the ribs that affects the effective exposure time of that region (see Harnden *et al.* 1984). Therefore we have not estimated an upper limit for source no. 1 and the count rate of source number 10 should be regarded as a lower limit.

Table 3 lists the average fluxes and luminosities for each source in the nominal Einstein band of 0.2–4.0 keV, obtained from the count rate in the merged image in the broad band. An identification of the X-ray sources with counterparts in M101, or foreground/background objects is also given in Table 3.

The total X-ray luminosity of M101, evaluated within the central 12′ radius, is $L_x \sim 1.2 \times 10^{40}$ ergs s^{-1} for the spectral parameters of Table 3, and for a 20% vignetting correction. About one-half of this luminosity is accounted for by the individual sources listed in Table 2. The residual counts are mostly clustered in the inner 5′ radius region, for a luminosity $L_x \sim 5 \times 10^{39}$ ergs s^{-1} for this inner disk component.[3] An average upper limit to the extended disk emission in the 5′–12′ region is evaluated at $L_x < 2.5 \times 10^{39}$ ergs s^{-1}, consistent with the estimate by McCammon and Sanders (1984), who evaluate it in a larger region ($r = 15'$).

Two sources are detected in the HRI observation near the galaxy center. However, they are detected only in the large detection cells, where the probability of detecting spurious sources is larger, and they do not coincide with the IPC peaks. It is possible that the HRI sources are simply fluctuations of the low intensity extended emission observed in the IPC.

ii) *Variability*

The count rate listed in Table 2 indicate that the intensity of five sources (numbers 4, 5, 8, 9, and 10) may have varied between the two observations, with variations of factors of ~1.5–2 up to 5 for source number 9. The 3 σ upper limit obtained from the I2141 data for source 10 is significantly lower than the count rate observed in I2140.

[3] The actual sum of the luminosities of individual sources within 12′, numbers 2, 4, 5, 8, and of the central 5′ region exceeds the total luminosity within 12′. However, each source luminosity includes a large correction (~33%) to account for the scattered photons outside the small detection cell, and the appropriate vignetting correction, which is a function of the source position in the field. No scattering correction has been applied to the luminosity of the whole galaxy.

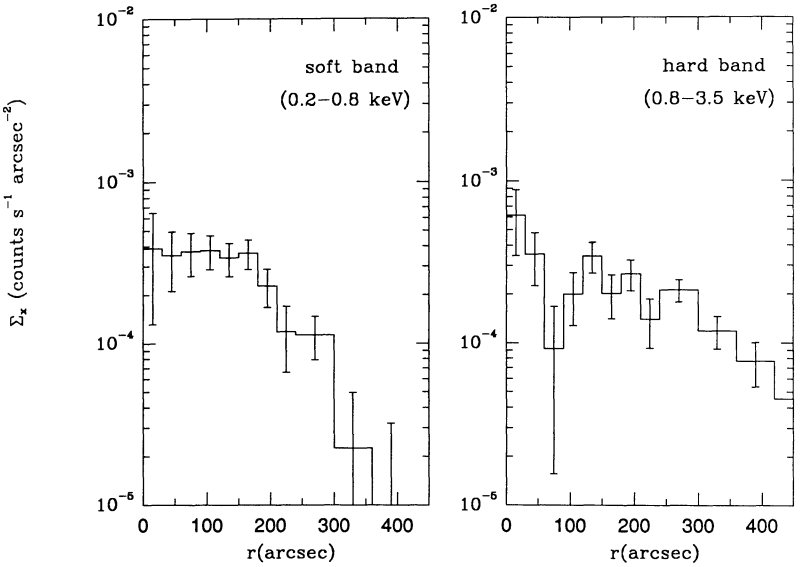

FIG. 3.—X-ray surface brightness distribution from the soft- and hard-energy bands from the merged IPC image

A quantitative comparison of the count rates and relative errors in the two observations ($|f_1 - f_2|/(\sigma_1^2 + \sigma_2^2)^{1/2}$) indicates that the difference in flux is significant at $\gtrsim 2\,\sigma$ for sources numbers 4, 5, at $\simeq 2.6\,\sigma$ for number 8, and $\sim 6\,\sigma$ for source number 9. Since this comparison cannot be done for source number 10, for which one observation gives only an upper limit, we have also used the method discussed by Maccacaro, Garilli, and Mereghetti (1987), that can be used in the presence of upper limits. This is based on Poisson statistics, and compares the observed counts in each observation with the counts expected from a source flux that varies within the observed values. A source is considered variable if at least in one of the observations the difference between observed and expected counts has a Poisson probability P of occurrence lower than a given threshold (10^{-3} for two observations, see Maccacaro, Garilli, and Mereghetti 1987).

Only two of the above sources comply with this criterion. We find $P \lesssim 1.7 \times 10^{-6}$ for source number 9, and $P \sim 2 \times 10^{-3}$ for source number 10 (although this is slightly higher than the threshold, it should probably be considered an upper limit, since the source is obscured by the IPC support structure in the first observation, see Table 2).

We have also looked at variability on smaller time scales, by binning the data into time intervals of approximately equal exposure and comparing the different bins. Each bin was $\sim$150, 250, 500, and 900 s long. This method does not give conclusive results for the first observation (I2140), because variability is also seen in four background regions devoid of sources, which were used as a control test. Even after a screening of the data with more stringent constraints, to eliminate a possible residual contamination from solar photons scattered off Earth surface, we could not obtain temporally stable background rates. The background level of the second observation (I2141) appears instead stable. We have found fluctuations in the flux level of sources numbers 6 and 8 when the I2141 data are binned in $\sim$900 s time intervals.

c) *Radial Profiles*

The X-ray emission in M101 is clumped in small regions and is mostly associated with individual objects (H II regions, OB complexes) in the galaxy. Its radial distribution therefore will be dominated by these discrete sources. The surface brightness radial profiles obtained from the merged image in the three energy bands are shown in Figures 3 and 4. In the absence of a strong central X-ray source, we have centered the profiles at $14^h01^m30^s$, 54°36′00″.

The soft profile is rather flat in the central 3′ and then decreases rapidly out to $\sim$5′. The distribution of the harder energy emission has a more irregular shape, which is due to the several individual sources, and extends further out, to $\sim$10′.

The broad-band X-ray and optical radial distributions are compared in Figure 4. The optical profile has been convolved with the IPC response to obtain the same angular resolution as the X-ray data. The two profiles have similar shapes, although

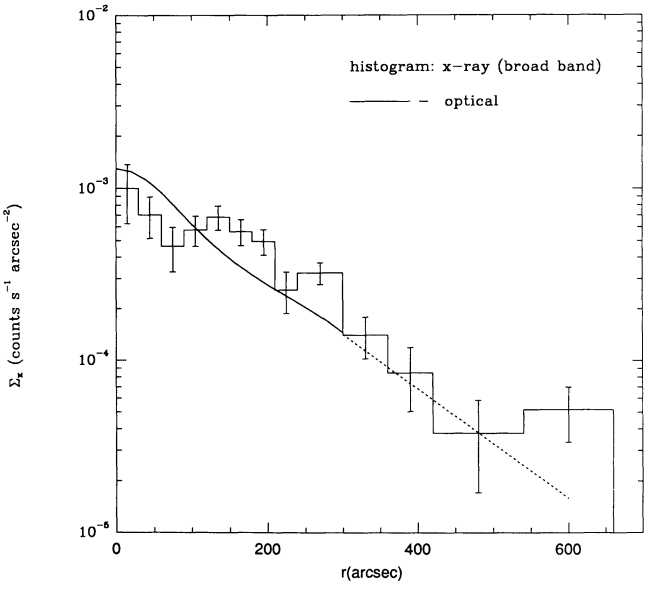

FIG. 4.—Comparison of the X-ray (broad-band) and optical radial distributions in M101. The optical data have been convolved with the IPC Response Function.

not as close as observed for other normal spiral galaxies (e.g., M83, Trinchieri, Fabbiano, and Palumbo 1985; M51; Palumbo *et al.* 1985; NGC 6946, Fabbiano and Trinchieri 1987; M33, Trinchieri, Fabbiano, and Peres 1988). This is probably due to the lack of a significant disk component in M101, relative to the more luminous sources. This component is most likely resulting from lower luminosity sources not resolved individually, tightly associated with the stellar population of the disk, and is observed in most other spirals (see Trinchieri, Fabbiano, and Peres 1988, and references therein). Thus in the M101 data, dominated by the individual source emission, the smooth exponential decay, typical of galactic disks, is not observed.

Profiles in the radio continuum and in the UV are also available for M101 (Gräve 1984; Hill, Bohlin, and Stecher 1984). As discussed by Hill, Bohlin, and Stecher, the light distribution in the UV bandpasses is similar to the optical-light distribution in the disk, with similar exponential scale lengths, and the comparison with the X-ray profile is thus equivalent. The radio continuum emission appears to have a shallower distribution than the optical or the X-ray emission, which would indicate a relative excess X-ray emission in the inner $\sim 3'$ region.

d) Spectral Fitting

A thermal bremsstrahlung spectrum with low energy cut-off has been fitted to the spectral distribution of the net counts within a 9′ radius circle centered on the galaxy. The background was estimated locally, in an adjacent annulus of 10′–14′, to ensure that source and background counts are observed at the same instrumental gain and that the real spectral distribution of the sky in the field is subtracted (a correction for small spatial gain variation is also taken into account; see Trinchieri, Fabbiano, and Canizares 1986; Fabbiano and Trinchieri 1987). Since with this choice we could have underestimated the background level, due to its radial dependence in the IPC (see Harnden *et al.* 1984), we have also corrected it, by increasing the background counts to match the level obtained from the background templates. We have analyzed each image independently, to take into account the different instrumental gains in the two observations. We have also repeated the analysis for the counts within $r = 5'$ region, to check for the possibility of a different spectrum in this inner region. The results are given in Table 4, and a plot of the confidence region for kT and N_H is shown in Figure 5.

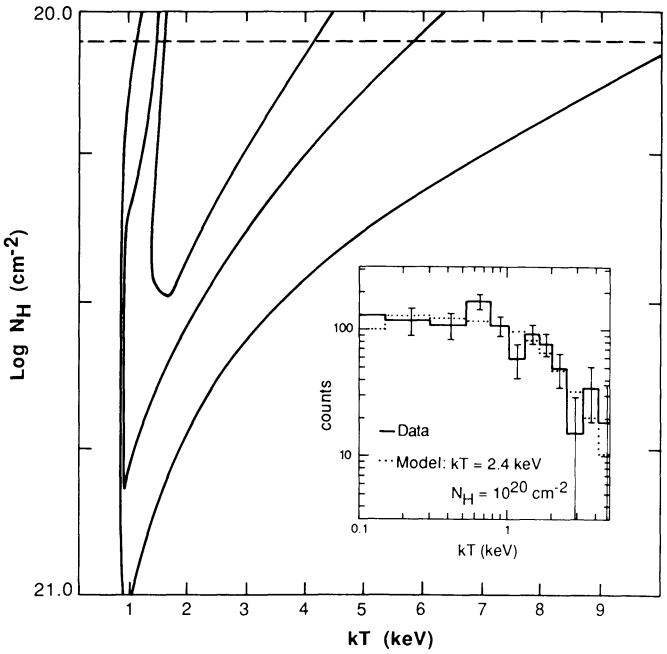

FIG. 5.—The 68%, 90%, and 99% confidence contours obtained from the fit of the spectral data of I2140 (longer observation) with a thermal bremsstrahlung spectrum with low-energy cut-off. The galactic N_H is indicated by the dashed line. The IPC spectral data and the best-fit spectrum are also shown.

The analysis of the two separate images gives consistent results. The spectral parameters are not well defined. We can put a lower limit to the temperature kT $\gtrsim 0.9$ keV, and N_H is consistent with the galactic value of $\sim 1.2 \times 10^{20}$ cm^{-2} (Stark *et al.* 1990). At the galactic N_H, the temperature can be constrained between kT ~ 1.5 and kT ~ 6. The inner 5′ region does not show a significantly different spectrum from the galaxy as a whole. Although not conclusive, the spectral results might indicate that M101 has a softer spectrum than the average spiral galaxy (see Fabbiano and Trinchieri 1987).

The net counts in each individual source in M101 are not enough to perform a detailed spectral analysis. Hardness ratios (HR), defined as the difference between hard- and soft-band counts, divided by the broad-band counts (obtained from a region of 3′ radius, to minimize the difference in the counts scattered outside of the source cell in the different energy

TABLE 4

SPECTRAL RESULTS

	I2140			I2141		
SOURCE RADIUS BKG RADIUS	NET COUNTS[a] ERROR	kT 90% confidence range (keV)	N_H 90% confidence range (cm^{-2})	NET COUNTS[a] ERROR	kT 90% confidence range (keV)	N_H 90% confidence range (cm^{-2})
0′–9′	849.5	2.4	1.0×10^{20}	439.3	0.9	1.2×10^{20}
10–14	±64.6	1.0–6.2	$<7.1 \times 10^{20}$	±46.2	0.8–3.0	$<4.0 \times 10^{20}$
0–9	645.5	0.9	5.0×10^{20}	303.0	0.9	1.0×10^{20}
10–14[b]	±66.5	0.9–9.0	$<3 \times 10^{21}$	±47.1	0.4–3.2	$<4 \times 10^{20}$
0–5	335.6	0.9	1.0×10^{20}	201.2	0.9	1.0×10^{20}
6–9	±36.8	0.7–3.0	$<3 \times 10^{20}$	±28.4	0.4–2.5	$<3 \times 10^{20}$

[a] Counts are obtained from the pulse-height analyzer channels corresponding to energies between 0.2–4.0 keV.

[b] The background level has been increased by 10% in I2140 and 15% in I2141 to match the levels from the background maps.

bands) have been determined for sources with a detection in both the hard and soft band. For source number 4, HR = 0.21 ± 0.11 in I2140 and 0.10 ± 0.15 in I2141. This is different from typical values for sources in galaxies (~ 0.5, see Fabbiano and Trinchieri 1987; Trinchieri, Fabbiano, and Peres 1988), and is closer to the hardness ratio of the inner 5′ region as a whole (0.07 ± 0.09 in I2140). However, the 3′ cell of source number 4 is likely to contain some of the unresolved emission from the galaxy. The hardness ratio of source number 8 (0.33 ± 0.24 in I2140; 0.52 ± 0.17 in I2141) is consistent with typical values of other galactic sources.

III. DISCUSSION

The main feature of the X-ray emission of M101 is its confinement into extremely bright, distinct point-like sources. A more extended component from the disk of the galaxy, generally observed in other spiral galaxies (e.g., M83, Trinchieri, Fabbiano and Palumbo 1985; M33, Trinchieri, Fabbiano, and Peres 1988; NGC 6946, Fabbiano and Trinchieri 1987), is not evident outside the inner 5′ region, although the upper limit to its luminosity is consistent with values observed in other systems. McCammon and Sanders (1984) suggest that as few as three point sources in the central region would appear as extended emission, when observed at the resolution of the IPC soft band in particular. The absence of a disk component in M101 might indicate a different luminosity function for the X-ray sources in M101, with a deficiency of lower luminosity sources compared to other spirals. We will address this issue later in the discussion.

The spectral characteristics of the galaxy as a whole might, in general, suggest a larger contribution from soft energy photons than in other spiral galaxies. Although the confidence region for the spectral parameters is consistent with that of other spirals, the shape of the confidence contours (Fig. 5) is different from that derived for a typical spiral spectrum (see Fabbiano and Trinchieri 1987), with the contour region open toward values of the absorbing column $N_{\rm H}$ lower than the galactic column density observed in H I. A similar behavior was also observed in the emission from the disk of M33, where a soft component, contributing mainly at energies below ~ 1 keV, was detected (Trinchieri, Fabbiano, and Peres 1988). If an equivalent component is present in M101, its intrinsic luminosity could be a factor of >10 higher than in M33. The quality of the present X-ray data however is not good enough to grant further speculation on this issue.

a) Bright Sources in M101

Five of the sources listed in Table 2 (numbers 2, 4, 5, 7, and 8) are likely to be in M101. They are on average much brighter than single X-ray sources detected in our Galaxy or in its nearby companions, as already noticed by Long and Van Speybroeck (1983). With the exception of the very bright binaries in the Magellanic Clouds (Clark *et al.* 1978), these sources have typically $L_x \lesssim 10^{38}$ ergs s^{-1}. The X-ray luminosity of each source in M101, calculated assuming a distance of 7.2 Mpc, exceeds in all cases 10^{38} erg s^{-1}, and can be as high as a few times 10^{39} ergs s^{-1}. It is unlikely that several equally bright objects contribute to the luminosity of each of these sources. The data suggest that the flux of these may vary in time (see § II*b*). Moreover, $\gtrsim 10$ sources with $L_x \sim 10^{38}$ would need to be clustered in each region. While the resolution of these observations cannot exclude this possibility, this would suggest that the X-ray sources in M101 show a higher degree of clustering than those of Local Group spirals. A fractional contribution from a more extended component in the plane of the galaxy cannot be entirely excluded; however, a large portion of the X-ray luminosity of each source is to be attributed to a single emitting object.

Overluminous sources are also observed in several other spirals (see Fabbiano and Trinchieri 1987; Fabbiano 1989). Different assumptions on the distances can, in some cases, reconcile the extreme luminosities with values observed in the Local Group galaxies. In the case of M101, we could match the high-luminosity end of the X-ray luminosity distribution of the sources in M31 or M33 only if we assume a distance for M101 lower than ~ 2 Mpc, which is below the lowest estimate of its distance (3.5 Mpc, Sandage 1962).

Most of the M101 sources are positionally associated with bright star-forming regions (Table 3). The association with the young stellar population of the galaxy, the high luminosities, and possible temporal variation, suggest that massive binary systems are the source of X-rays. The extreme X-ray luminosities are all above the Eddington limit for a 1 $M_\odot$ object ($\sim 1 \times 10^{38}$ ergs s^{-1}) even for the lowest estimate of the distance, indicating that the collapsed object is probably not a neutron star, but more likely is a massive black hole, with $M \gg 1\ M_\odot$.

Although most of the M101 sources are associated with star-forming regions (see Table 3), only NGC 5447 of the brightest H II regions has been detected in X-rays. For the other regions, we have estimated 3 σ limits of $L_x \sim 4$–8×10^{38} ergs s^{-1}, depending upon the location of the region in the IPC field. These limits are similar to the X-ray luminosity of the source observed in NGC 5447, and are high enough that a bright binary source could still be present and be below the detection threshold in our observations. However, if every one of the ~ 200 H II regions in the plane of the galaxy (Hodge 1969) contained one such source, its average luminosity would have to be lower than $\sim 5 \times 10^{37}$ ergs s^{-1}, otherwise the integrated emission of all H II regions would be evident as a lower surface brightness emission in the plane. Therefore, either only a few of the H II regions in M101 contain evolved X-ray emitting binary sources, or there is a discontinuity in the luminosity distribution of the X-ray sources in M101, with a deficiency of sources in the range of $L_x \sim 10^{37-38}$ ergs s^{-1}.

b) Luminosity Distribution of the X-Ray Sources in M101

To further investigate the issue of the luminosity distribution of the M101 sources (in the assumption that each detected source is indeed a single object), we compare in Figure 6 the luminosity distribution of the X-ray sources in the disk of M31 (Trinchieri *et al.* 1990), M33 (Trinchieri, Fabbiano and Peres 1988) and M101, binned in 4 logarithmic bins per decade. The latter two galaxies have similar morphologies (both are Sc galaxies), although M101 is ~ 30 times more luminous in X-rays than M33 (if we exclude the nuclear source in the latter), and similarly more luminous in the optical. A similar comparison, between M31 and M81, both of earlier morphological type, was done by Fabbiano (1988).

M31 provides, so far, the best estimate of the luminosity distribution of X-ray sources in spiral disks. This can be represented by a single power law with slope between ~ -0.6 and -1.0 (representing the 68% confidence region extremes), truncated at $L_x \sim 1$–5×10^{36} ergs s^{-1}, in order not to exceed the total disk luminosity (see Fabbiano 1988; Trinchieri *et al.* 1990). These two functions are reproduced in Figure 6 on the

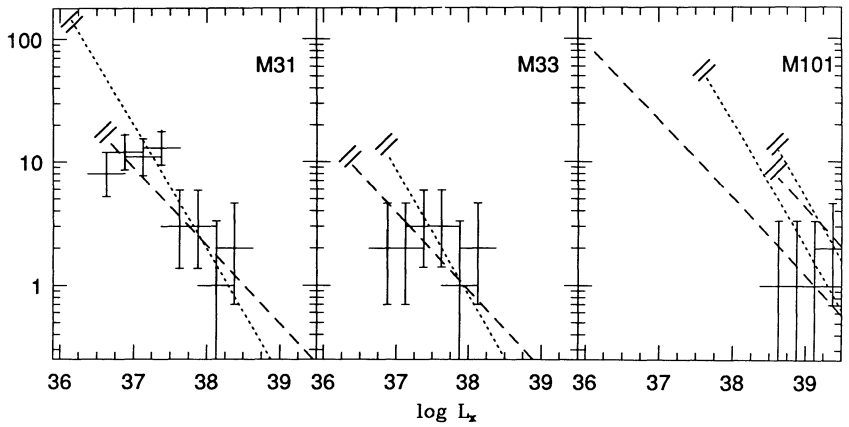

FIG. 6.—The luminosity distribution of the X-ray sources in M31 (from Trinchieri *et al.* 1990), M33 (from Trinchieri, Fabbiano, and Peres 1988) and M101. Power laws with slopes −1.0 and −0.6 are fitted through the points. The power laws are truncated at the turnover luminosities (*see text*).

M31 data, and are also normalized to the data for the other galaxies. It is clear that these power laws are consistent with the M33 points, although a flatter power law cannot be ruled out.

Given the poor statistical significance of the M101 data, the normalization of these power laws to the M101 points spans a rather large range. In Figure 6 we show the extreme cases for which the power-law functions go through at least the two points at higher luminosity (within the 68% error, estimated from Gehrels 1986). With this constraint on the normalization, there is only a small range in the parameter space that allows a truncation at luminosities around or below $L_x \sim 10^{37}$ ergs s^{-1}; in most cases, the power-law functions need to be truncated at $L_x \gtrsim 10^{38}$ ergs s^{-1}. These values are higher than the corresponding turnover luminosities in both M33 and M31 (and also M81, see Fabbiano 1988).

Although the present data only allow tentative conclusions, they still suggest the following:

1. If a "universal" luminosity function, i.e., a power-law distribution $N \propto L^{-\alpha}$ with similar exponents and low-luminosity cut-offs, explains the luminosity distribution of X-ray sources in *all* spiral galaxies, α should have values between 0.6–0.8. Larger/brighter galaxies would then simply contain more sources, and the higher normalization would naturally allow an extension of the function at high luminosities.

2. Luminosity functions with $\alpha \lesssim 0.6$ could explain the M101 (and M33) data, but would not represent those of M31. These flat luminosity functions will moreover require a rather narrow range in the normalization parameter, to explain the whole of the emission with discrete sources. Alternatively, the luminosity function either steepens at lower luminosities, or different components, other than discrete sources, must contribute to the total X-ray luminosity observed. However, there is no evidence of significant extended emission that could originate from a hot phase of the interstellar medium in M101 (see McCammon and Sanders 1984).

3. If we release the assumption of one luminosity function for all spiral galaxies, then it is possible that in M101, and to a lesser degree in M81 (Fabbiano 1988), there is a deficiency of intermediate/lower luminosity sources (of $\sim 10^{37}$–10^{38} ergs s^{-1}) relative to high luminosity ones. Although the normalization parameter is highly uncertain, it would seem that power laws appropriate for the M31 data would need to be truncated at $L_x > 10^{37}$ ergs s^{-1}, in order not to exceed the observed total luminosity. We could then have a situation in which, on top of a distribution of X-ray sources similar to that of M31 (most of which would fall below the detection threshold in M101), there is another distribution of much brighter sources (that we detect), truncated at $L_x > 10^{38}$ ergs s^{-1}. This conclusion could be supported by the suggestion of Blitz *et al.* (1981) that OB star-formation efficiency in NGC 5461, one of the brightest H II regions in M101, is higher than in galactic molecular cloud complexes, which might then favor the formation of bright, very massive binary systems, progenitors of the high-luminosity X-ray sources. Moreover, very massive stars ($> 50\ M_\odot$) are likely to be present in these regions, as suggested by the association between H II regions and Type II supernovae observed in M101 (Richter and Rosa 1984). A similar conclusion was reached from the radio observations of the H II complexes. A comparison with M33, whose brightest regions are a factor ~ 50 fainter than in M101, led Israel, Goss, and Allen (1975) to suggest that there are two luminosity distributions, a steep one with a cut-off at very high flux levels superposed onto a distribution similar to that of M33. Very high masses could lead to black holes, rather than neutron stars, in binaries, which would perhaps be consistent with the higher L_x observed.

If each of the bright M101 sources is in reality a cluster of several equally luminous objects, the above discussion does not apply. In this case, we can assume that the source luminosities are really distribution like the M31 or M33 sources, with a higher normalization reflecting the larger total X-ray luminosity of M101. Either of the M31 slopes would be compatible with the total M101 luminosity if they are truncated at $L_x \sim 10^{37}$ ergs s^{-1}.

IV. CONCLUSIONS

The X-ray image of M101 shows an extended feature at the galaxy's center, and several sources in the disk. The luminosity of each source is well above $L_x \sim 10^{38}$ erg s^{-1}, and they are most likely individual massive binary systems, with a $M \gg 1$ $M_\odot$ collapsed object. Although the present data do not allow us to reach strong conclusions, they suggest a deficiency of sources with $L_x \sim 10^{37-38}$ ergs s^{-1} in M101, by comparison with the M31 disk. This could either be due to a luminosity function for X-ray sources flatter than in M31, or to a popu-

lation of very massive and very young stars in H II regions, possibly superposed onto a population similar to that of the M31 disk, that could explain the excess of very bright X-ray sources in this galaxy. Future, more sensitive X-ray data are, however, strongly needed to confirm the above conclusions.

The data used in this paper are all from the *Einstein* Data Bank. We thank S. Hazelton for helping us with the reduction of the data. G. T. acknowledges financial support by the Agenzia Spaziale Italiana. This work was supported by NASA contract NAS8-30751.

REFERENCES

Allen, R. J., and Goss, W. M. 1979, *Astr. Ap. Suppl.*, **36**, 135.
Blitz, L., Israel, F. P., Neugebauer, G., Gatley, I., Lee, T. J., and Beattie, D. H. 1981, *Ap. J.*, **249**, 76.
Bottinelli, L., and Gouguenheim, L. 1976, *Astr. Ap.*, **51**, 275.
Clark, G., Doxsey, R., Li, F., Jernigan, J. G., and Van Paradjis, J. 1978, *Ap. J. (Letters)*, **221**, L37.
Cox, D. P., and McCammon, D. 1986, *Ap. J.*, **304**, 657.
Fabbiano, G. 1988, *Ap. J.*, **325**, 544.
———. 1989, *Ann. Rev. Astr. Ap.*, **27**, 87.
Fabbiano, G., and Trinchieri, G. 1987, *Ap. J.*, **315**, 46.
Gehrels, N. 1986, *Ap. J.*, **303**, 336.
Giacconi, R., *et al.* 1979, *Ap. J.*, **230**, 540.
Gräve, R. 1984, Ph.D. thesis, University of Bonn.
Harnden, F. R., Fabricant, D. G., Morris, D. E., and Schwarz, J. 1984, Internal SAO Special Report No. 393.
Hill, J. K., Bohlin, R. C., and Stecher, T. P. 1984, *Ap. J.*, **277**, 542.
Hodge, P. W. 1969, *Ap. J. Suppl.*, **18**, 73.
Hutchmeier, W. K., and Witzel, A. 1979, *Astr. Ap.*, **74**, 138.
Israel, F. P. 1980, *Astr. Ap.*, **90**, 246.
Israel, F. P., Goss, W. M., and Allen, R. J. 1975, *Astr. Ap.*, **40**, 421.
Long, K., and Van Speybroeck, L. P. 1983, *Accretion-Driven Stellar X-Ray Sources*, ed. W. H. G. Lewin and P. J. Van Den Heuvel (Cambridge: Cambridge University Press), p. 117.
Maccacaro, T., Garilli, B., and Mereghetti, S. 1987, *A.J.*, **93**, 1484.
Margon, B., Downes, R. A., and Chanan, G. A. 1985, *Ap. J. Suppl.*, **59**, 23.
McCutcheon, W. H. 1973, *A.J.*, **78**, 18.
McCammon, D., and Sanders, W. T. 1984, *Ap. J.*, **287**, 167.
Palumbo, G. G. C., Fabbiano, G., Fransson, C., and Trinchieri, G. 1985, *Ap. J.*, **298**, 259.
Richter, O.-G., and Rosa, M. 1984, *Astr. Ap.*, **140**, L1.
Sandage, A. 1962, *IAU Symposium*, **15**, 359.
Sandage, A., and Tamman, G. A. 1974, *Ap. J.*, **194**, 223.
Searle, L. 1971, *Ap. J.*, **168**, 327.
Stark, A. A., Heiles, C., Bally, J., and Linke, R. 1990, in preparation.
Topka, K. *et al.* 1982, *Ap. J.*, **259**, 677.
Trinchieri, G. *et al.* 1990, in preparation.
Trinchieri, G., Fabbiano, G., and Canizares, C. R. 1986, *Ap. J.*, **310**, 637.
Trinchieri, G., Fabbiano, G., and Elvis, M. 1989, *Ap. J.*, submitted.
Trinchieri, G., Fabbiano, G., and Palumbo, G. G. C. 1985, *Ap. J.*, **290**, 96.
Trinchieri, G., Fabbiano, G., and Peres, G. 1988, *Ap. J.*, **325**, 531.
Vaiana, G. S., *et al.* 1981, *Ap. J.*, **245**, 163.

G. FABBIANO, S. ROMAINE, and G. TRINCHIERI: Center for Astrophysics, 60 Garden Street, Cambridge, MA 02138